Performance evaluation of a R-290 dual-source heat pump for heating and cooling

Laura Alonso [a], Xabier Peña [a], Felipe Trebilcock [a], Julen Hernandez [a], Aitor Agirre [a]

[a] Efficient Thermal Energy Systems / Energy, Climate and Urban Transition / TECNALIA, Basque Research and Technology Alliance (BRTA). Azpeitia, Spain. laura.alonso@tecnalia.com

Abstract. In this paper, the performance of a 10 kW reversible heat pump using R290 as refrigerant and using a dual source/sink is presented. The heat pump design is oriented for its integration with solar photovoltaic energy in multifamily near Zero Energy Buildings, with the objective to reach a high onsite renewable share. The development is part of TRI-HP project: Trigeneration systems based on heat pumps with natural refrigerants and multiple renewable sources. The heat pump has a specifically designed dual source heat exchanger (DSHX) working as the outdoor unit of the heat pump. This element is able to work as a condenser (cooling mode) or evaporator (heating mode), exchanging heat between the refrigerant and air or water/brine as heat source (in heating mode) or sink (in cooling mode). Both sources can also be simultaneously used as heat source or sink. The design procedure and used correlations for the DSHX are described. The heat pump has been experimentally tested in a climatic chamber in all the possible different working modes (Heating with air, heating with brine, cooling with air, cooling with brine), showing in general a good agreement with the design values. Results for coefficient of performance, heating/cooling capacities and compressor consumption are presented for different air/brine temperatures and different compressor velocities. The experimental campaign has served to validate the developed models for designing the DSHX. Future work includes an improved redesign of the heat pump with a more compact DSHX and a simplified refrigerant circuit, which will be experimentally tested in an analogous experimental campaign.

Keywords. Dual-source, heat exchanger, heat pump, R290.
DOI: https://doi.org/10.34641/clima.2022.381

1. Introduction

According to the Roadmap to a Resource Efficient Europe, Europe must reduce its greenhouse gas emissions by 80-95% by 2050 [1]. Cities and the construction sector play a decisive role in the process of energy transition and reduction of the carbon footprint in the EU. Within this context, the generation of heat and cold in buildings can and should play an important role towards the change of model.

Heat pumps have characteristics that make them very interesting for use in near-zero energy buildings (EECN). These buildings are designed to have a very low energy demand, which is largely covered by energy from renewable sources, including self-production of renewable energy. In this context and considering residential energy consumption, the heat pump is imposed as a technology for the future. Due to its consideration of renewable, versatility and high energy efficiency, the development of heat pump technology will be crucial in this transition towards almost zero energy buildings.

The use of low-impact refrigerants is a need that is already covered by regulations, and is expected to increase in the future. This is due to the fact that traditional refrigerants have a high global warming potential (GWP), and their use has begun to be restricted for certain applications. The F-Gas regulation [2] has determined a series of restrictions on the use of refrigerants until the year 2030. As of January 1, 2022, fluorinated gases with a GWP ≥ 150 will be prohibited in sealed commercial equipment except equipment for evaporation <-50 °C or with a fluid load less than 40 tCO2eq. In this context, the use of natural refrigerants is spreading in cases where it is technologically safe and economically feasible.

The use of dual systems combining geothermal and aerothermal is considered an innovative alternative to the use of aerothermal or geothermal heat pumps [3]. Jin et al. [4] analysed the potential of a hybrid system combining ambient air and geothermal energy, obtaining COP improvements of 28.1% and 4.7% for the system in heating and cooling operating modes, respectively. Man et al. [5] presented simulations of a hybrid

Copyright ©2022 by the authors. This conference paper is published under a CC-BY-4.0 license.

aerothermal/geothermal system, with supplemental air sinks for a residential building in Hong Kong. The economic analysis showed a savings in investment costs of 34.3% compared to a conventional geothermal system; with a saving in operating costs of 53.6% in a period of 10 years.

However, all current hybrid aerothermal/geothermal systems use two exchangers in parallel, a cooling-air exchanger (coil) and a cooling-water/brine exchanger (geothermal exchanger). In this project, the designed heat pump performs the exchange with both energy sources in the same device, the dual heat exchanger.

2. Dual-source heat pump design

2.1 Dual-source heat pump concept and system integration

The designed dual-source heat pump (DSHP) uses R290, a natural refrigerant, and is envisaged to be integrated in multi-family residential buildings, and be powered by largely renewable electricity (from photovoltaic panels with battery electrical storage). Fig. 1 shows a diagram of the proposed heat pump integrated into the building's thermal system.

The heat pump is equipped with a space conditioning heat exchanger (SCHX) and a desuperheater (DSH) in the demand side, and can provide heating or domestic hot water (DHW) using both exchangers or use them simultaneously to provide both services at different temperatures. It also allows the provision of cooling and DHW simultaneously, thanks to the use of the compressor discharge heat in the DSH. The external heat exchanger, which is dual-source, allows the use of geothermal and/or aerothermal energy, depending on the most favourable conditions. In addition, the system allows free cooling directly from the ground. It is, therefore, a versatile system which makes possible multiple modes of operation.

The main innovation of the heat pump is the use of a dual-source heat exchanger (DSHX) in the source/sink side. This feature of the heat pump allows the length of the geothermal boreholes to be reduced by around 50% compared to a conventional geothermal heat pump system, which leads to considerable savings in investment costs.

2.1 Dual-source heat exchanger design

A DSHX has been designed such that it can exchange heat with the water/brine (ground), air or with both simultaneously depending on environmental conditions. Moreover, the design allows to use this heat exchanger as evaporator or condenser in order to reverse the heat pump cycle. The working modes of the DSHX include:

- **Heating air-water.** DSHX working as an evaporator, exchanging heat between air and R290.
- **Cooling air-water.** DSHX working as a condenser, exchanging heat between air and R290.
- **Heating water-water.** DSHX working as an evaporator, exchanging heat between water and R290.
- **Cooling water-water.** DSHX working as a condenser, exchanging heat between water and R290.

The geometry of the DSHX consists on an external air finned coil with an internal coaxial bare tube. The air exchanges heat with the refrigerant, which flows through the annular space between the two coaxial tubes. The water flows through the inside of the internal tube, therefore being able to exchange heat with the refrigerant. A scheme of the DSHX is shown in Fig. 2.

In order to perform the design, four different design tools, each one corresponding to the working modes of the DSHX, have been defined for determining the capacity of each working mode and it's required heat exchange surface. The dimensioning tools have been implemented as deterministic models in EES (Engineering Equation Solver) [6] based on the geometry of each heat exchanging part:

- Geometry of air source heat exchanger or coil, for air source/sink evaporator/condenser and,
- Geometry of coaxial tube heat exchangers, for geothermal source/sink evaporator/condenser.

Wang et al. [7] correlation has been used to calculate the air side heat transfer coefficient of the DSHX.

Different correlations have been used for the sensible heat transfer coefficient on the refrigerant side and on the water side of the DSHX, depending on the regime:

- Correlation proposed by Shah and London [8] for laminar regime (Re < 2300).
- An interpolation between results for laminar flow and turbulent flow is applied for transitional flow (2300<Re<3000), as proposed by Nellis and Klein [9].
- Correlation proposed in VDI Heat Atlas [10] for Re numbers between 3000 and 10000.
- Correlation of Dittus-Böelter [11] for turbulent regimes (Re > 10000).

For the calculation of the HTC in the condensing zone the correlation recently proposed by Shah [12,13] has been implemented.

On the other hand, the correlations proposed by Mishima et al. [14] and Shah [15] have been implemented for the evaporation zone.

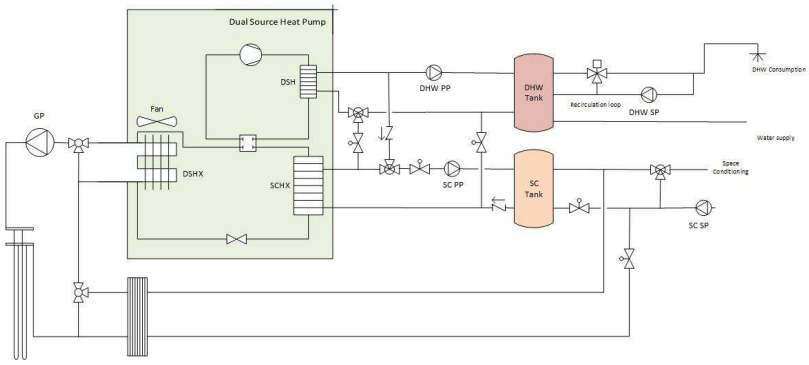

Fig.1 - DSHP integrated into the building's thermal system.

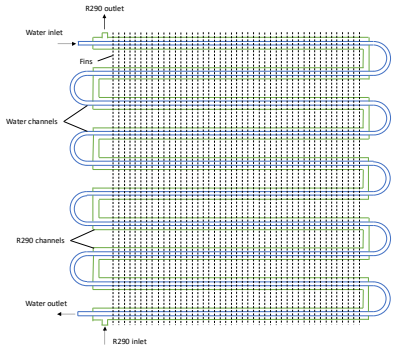

Fig.2 – DSHX scheme.

3. Dual-source heat pump testing

The R290 DSHP prototype has been experimentally tested inside a climatic chamber in the laboratory (Fig. 3). The main achievements of the first testing campaign have been:

- Measuring heat pump capacity and efficiency for different operation modes.
- Generating data for testing a simple heat pump model for further simulations.
- Detecting problems and potential for optimization.

The climatic chamber of the laboratory can be partitioned into two chambers, having two symmetric dissipation and energy producing systems, which can work at the same conditions when the chamber is unique, or separately at independent conditions when it is separated in two chambers. The DSHP prototype is located in Chamber number one (hereinafter Chamber1), which contains the following dissipation and energy generation equipment:

- 5 impeller pumps. Impulsion pump number 2 (hereinafter Pump2), is the one which is linked to the demand side of the HP, and will provide the water flow rate to the SCHX (at heating, cooling and DWH modes) and the DSH (at heating, heating+DHW, cooling+DHW modes).
- 3 heat exchangers.
- A 885 l buffer tank.

Fig.3 - DSHX test bench installed inside the climatic chamber.

Fig. 4 shows the scheme of Chamber1, where the DSHX test bench has been installed. In order to reach to the desired testing conditions in Chamber1, an Air Handling Unit (AHU) is used. The AHU comprises different heat exchanging coils. In the AHU, two fans blow the air coming from the chamber through the heat exchanging coils until it is expelled uniformly through hoppers. The air is treated in the different heat exchanging coils inside the AHU, achieving the desired conditions.

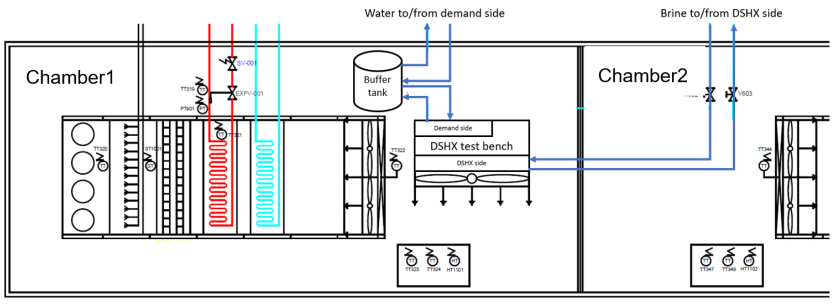

Fig.4 – Scheme of the DSHX test bench installed in the climatic chamber.

As the DSHX can work with air or water/brine, it needs to be connected to another heat source/sink, so a connection with Chamber number two (hereinafter Chamber2) was implemented, providing a water flow rate to the DSHX. Air conditions and demand side conditions are controlled from Chamber1; DSHX source/sink conditions when it is working with water/brine, are controlled from Chamber2. A buffer tank of 250 l was installed between the test bench and the demand side circuit to gain stability. Inside Chamber1 there are two sensors, an NTC sensor for measuring ambient dry bulb temperature, and a relative humidity sensor. Besides these two sensors, the additional metering instrumentation shown in Table 1 has been included for the testing of the unit. During the initial tests, the PIDs of the climatic chamber have been adjusted in order to get the maximum possible stability in the measurements.

Testing has been conducted following EN 14511 procedures [16], in the different possible working modes. Fist, the room is preconditioned and when the required tolerances are met, it is maintained in steady-state operation for sufficient time, then calculating the heating and cooling capacities based on the measurements on the demand-side fluid (water).

• **Heating air-water.** The DSHP was tested for 7 °C ambient air temperature, producing warm water from 30 °C to 35 °C, from 40 °C to 45 °C, from 47 °C to 55 °C and from 52 °C to 60 °C. The testing campaign was developed with the compressor at its nominal operating point, 70 rps, and at different partial loads: 50 rps, 60 rps and 90 rps (full load).

• **Cooling air-water.** The DSHP was tested for different ambient temperatures: 27 °C, 35 °C and 45 °C; chilling water from 12 °C to 7 °C and from 23 °C to 18 °C, at its nominal operating point with compressor working at 70 rps and at different partial loads: 40 rps, 50 rps, and full load 90 rps.

• **Heating water-water.** The DSHP was tested for different water source temperatures: 7 °C, 12 °C and 16 °C; producing warm water at 35 °C and 45 °C. Several compressor speeds have been tested, from 50 rps to 90 rps.

• **Cooling water-water.** The DSHP was tested for different water sink (rejection) temperatures: 25 °C and 30 °C. A cold-water supply from 12 °C to 7 °C was tested. The compressor speed varied from its nominal operating point at 70 rps, to different partial loads at 50 rps, 60 rps, and full load 90 rps.

4. Results and discussion

In the following subsections the achieved experimental results are presented for each working mode in all the testing points defined. The experimental values have not been compared for the different sources, as the idea behind the dual-source heat pump is to switch between one mode (air as source/sink) or the other (brine as source/sink) depending on the external conditions, mainly air temperature as the ground temperature is going to be more constant. Also, for the same experimental points (same temperatures with air and with brine), quite similar performance is encountered for air/brine modes.

4.1 DSHP in heating mode using air as heat source

Heating capacity, measured at SCHX, and Coefficient of Performance (COP) are increasing with decreasing SCHX water supply temperature, therefore reducing the pressure ratio / required temperature boost, as can be seen in Fig. 5 and Fig. 6. Fig. 7 shows the compressor electrical power in the different testing conditions. On the one hand, the highest heating capacity values at SCHX and electrical consumption values are achieved with the highest compressor speed. On the other hand, the highest cycle efficiencies are achieved with the lowest compressor speed. The calculated COP for high supply temperatures is around 2.5, which is rather low.

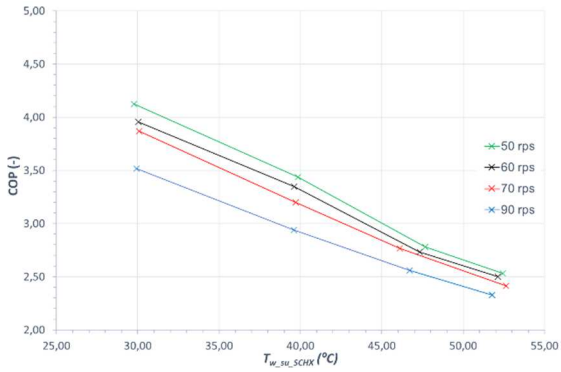

Fig.5 – COP for different water supply temperatures to the SCHX and compressor speeds (rps). Heating air-water mode.

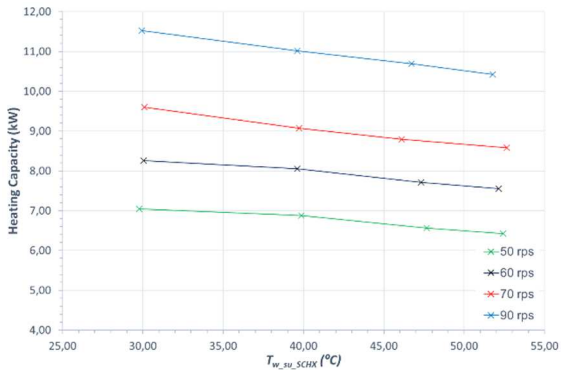

Fig.6 – Heating capacity for different water supply temperatures to the SCHX and compressor speeds (rps). Heating air-water mode.

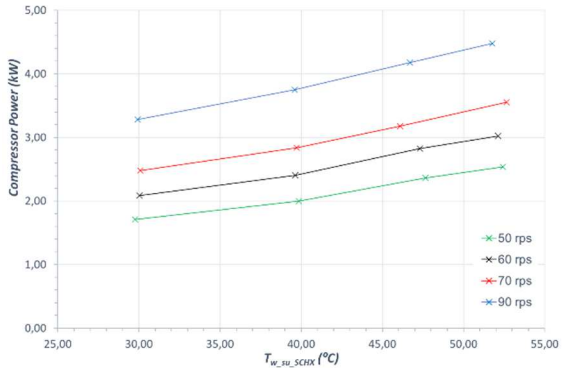

Fig. 7 – Compressor power for different water supply temperatures to the SCHX and compressor speeds (rps). Heating air-water mode.

This is due to abnormal refrigerant pressure drop on the DSHX, observed when the device is working in heating mode. This leads to lower values than predicted with the developed models.

Fig. 8 shows the deviation between the DSHX capacity estimated by the dimensioning tool and the experimental results. The deviation is below 10 % for all of the testing points. Therefore, the numerical model can be used for predicting the capacity of the DSHX as air source evaporator. The capacity calculated with the thermodynamic model is obtained by introducing correction factors which account for the refrigerant pressure drop values obtained experimentally.

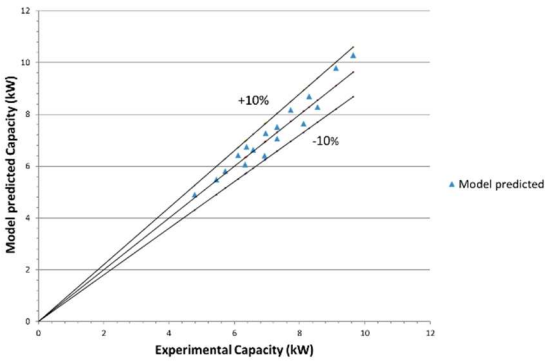

Fig.8 – Capacity deviation between thermodynamic model and tested values for DSHX working as evaporator with air.

4.2 DSHP in cooling mode using air as heat sink

Cooling capacity at SCHX and Energy Efficiency Ratio (EER) are increasing with decreasing ambient temperature, therefore reducing the pressure ratio / required temperature boost, as can be seen in Fig. 9 and Fig. 10.

Fig. 11 shows the compressor electrical power in the different testing conditions. On the one hand, the higher the compressor speed, the larger the cooling power and electrical consumption values. On the other hand, the lower the compressor speed, the higher the cycle efficiency. Nevertheless, the EER values achieved with low compressor velocities 40 and 50 rps are really close. The calculated COP for high ambient temperatures is between 2.5 to 3.2, aligned with the expected values. As expected, the highest the ambient temperature, the lower the cooling capacity in the SCHX, due to the higher pressure-ratio.

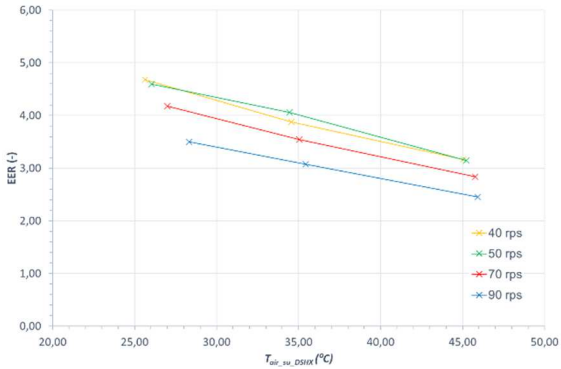

Fig.9 – EER for different water supply temperatures to the DSHX and compressor speeds (rps). Cooling air-water mode, producing cooling from 12 °C to 7 °C.

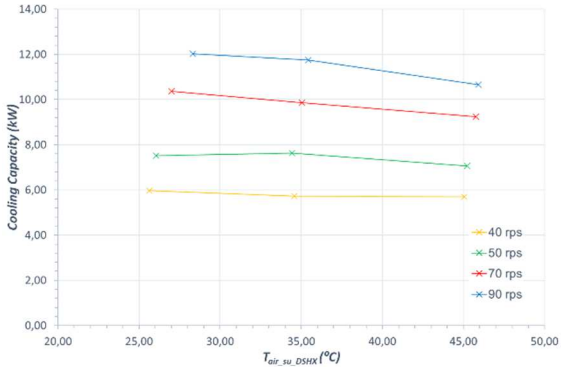

Fig.10 – Cooling capacity for different water supply temperatures to the SCHX and compressor speeds (rps). Cooling air-water mode, producing cooling from 12 °C to 7 °C.

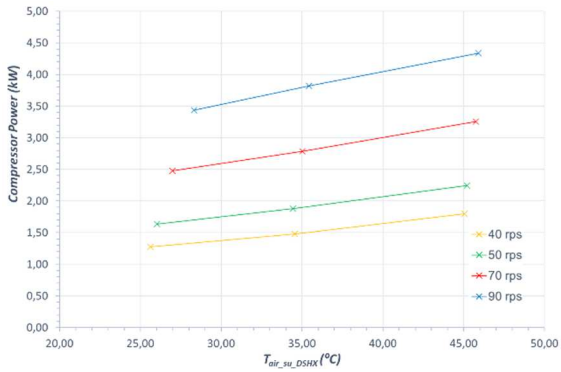

Fig.11 – Compressor power for different water supply temperatures to the SCHX and compressor speeds (rps). Cooling air-water mode, producing cooling from 12 °C to 7 °C.

Fig. 12 shows the deviation between the condenser capacity estimated by the dimensioning tool and the experimental results. The model tends to slightly over-predict the behavior of the DSHX in air

condenser mode, but deviations below 10 % are found for all the testing points, and are considered acceptable.

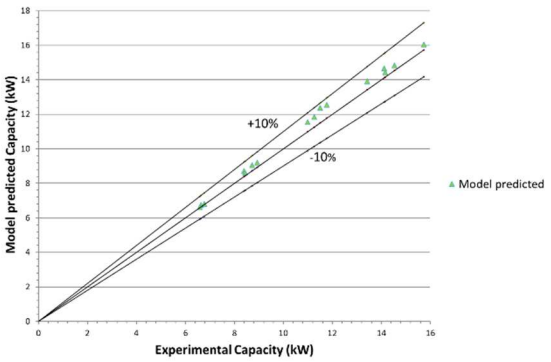

Fig.12 – Capacity deviation between thermodynamic model and tested values for DSHX working as condenser with air.

4.3 DSHP in heating mode using water as heat source

Tendencies showing the influence of compressor speed on the COP can be observed in Fig. 13, and on the heating capacity in Fig. 14, for different DSHX water/brine supply temperatures and maintaining the SCHX supply temperature at 40 °C for all cases represented. Fig. 15 shows the compressor electrical power in the different testing conditions. DSHP heating capacity and electricity consumption increase as compressor speed increases, achieving higher capacities when the pressure ratio is reduced. Respect to the DSHP efficiency, the lower the pressure ratio, the higher the achieved COP values. In addition, the lower the compressor speed, the higher the COP.

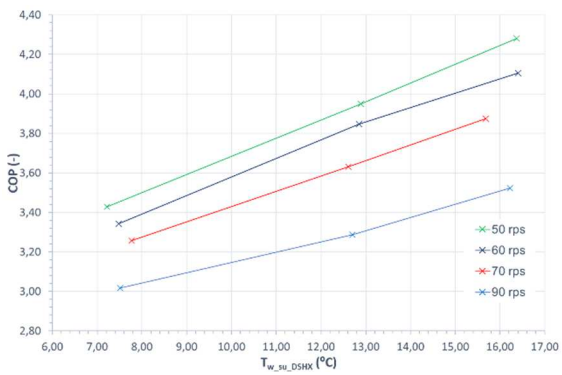

Fig.13 – COP for different water supply temperatures to the DSHX and compressor speeds (rps). Heating water-water mode, producing heating from 40 °C to 45 °C.

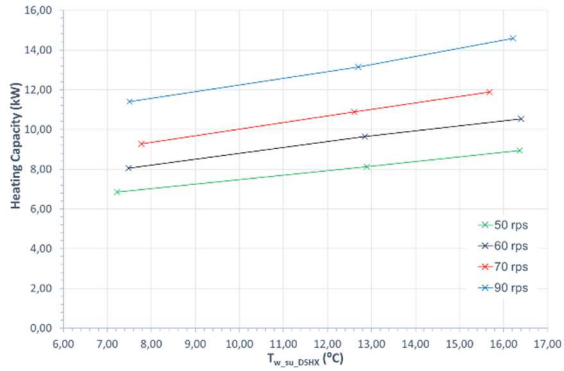

Fig.14 - Heating capacity for different water supply temperatures to the DSHX and compressor speeds (rps). Heating water-water mode, producing heating from 40 °C to 45 °C.

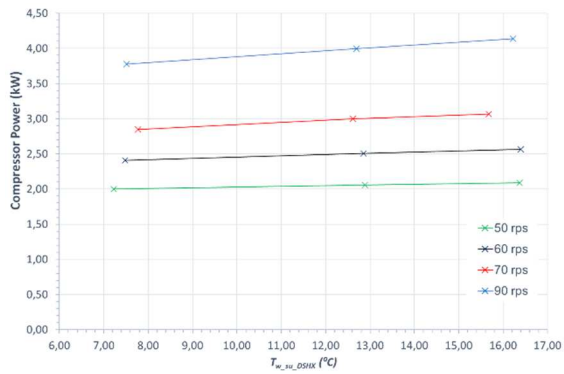

Fig.15 - Compressor power for different water supply temperatures to the DSHX and compressor speeds (rps). Heating water-water mode, producing heating from 40 °C to 45 °C.

Fig. 16 shows the deviation between the evaporation heat obtained by the numerical model and the experiments. As can be seen the deviation is below 10% for all of the testing points. Therefore, the numerical model predicts the evaporation heat with a good accuracy and could be used as dimensioning tool.

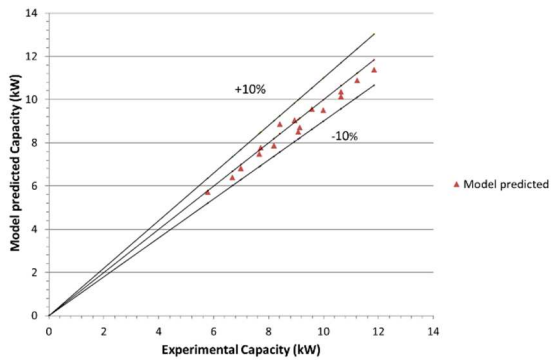

Fig.16 – Capacity deviation between thermodynamic model and tested values for DSHX working as evaporator with water.

4.4 DSHP in cooling mode using water as heat source

EER values increase when DSHX supply stream temperatures decrease, therefore reducing the pressure ratio / required temperature boost, as can be seen in Fig. 17. But this enhancement is only due to the higher compressor electricity consumption, because the cooling capacity seems to remain constant for both DSHX supply temperatures, as can be observed in Fig. 18. On the one hand, the higher the compressor speed, the larger electrical consumption, as can be seen in Fig. 19. On the other hand, the lower the compressor speed, the higher the cycle efficiency (EER), but not for 50 rps at 25 °C DSHX supply temperature. Nevertheless, the EER values achieved with low compressor velocities, 50 and 60 rps are really close at 30 °C DSHX water supply temperature. The calculated EER values for high water supply temperature (30 °C) are between 3.2 to 3.8, aligned with the expected values.

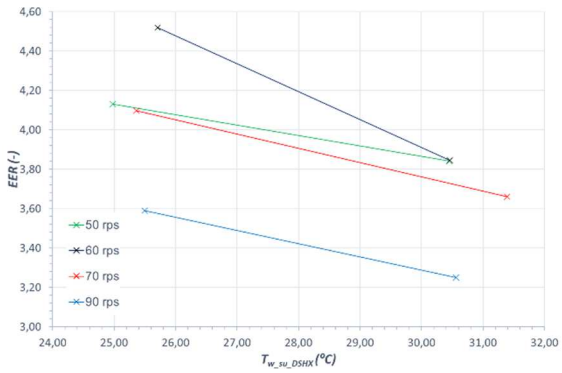

Fig.17 – EER for different water supply temperatures to the DSHX and compressor speeds (rps). Cooling water-water mode, producing cooling from 12 °C to 7 °C.

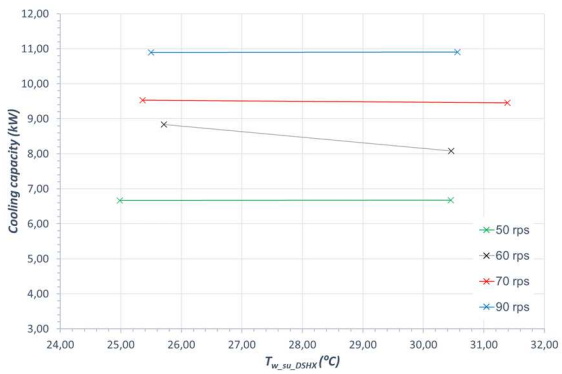

Fig.18 - Cooling capacity for different water supply temperatures to the DSHX and compressor speeds (rps). Cooling water-water mode, producing cooling from 12 °C to 7 °C.

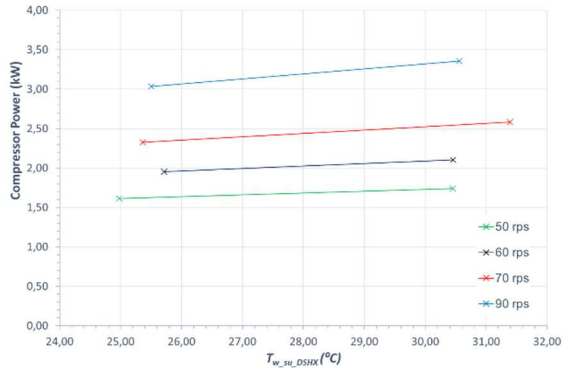

Fig.19 - Compressor power for different water supply temperatures to the DSHX and compressor speeds (rps). Cooling water-water mode, producing cooling from 12 °C to 7 °C.

Fig. 20 shows the comparison between the model predicted capacity and the experimental values, showing deviations for the same testing conditions below 15% for all the points tested. The model overpredicts slightly the behaviour of the DSHX at ground source condenser mode, but the difference could be considered acceptable.

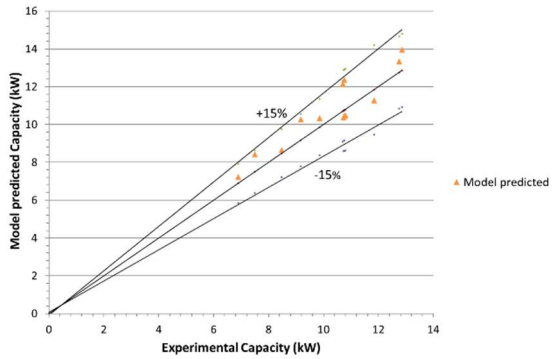

Fig.20 – Capacity deviation between thermodynamic model and tested values for DSHX working as condenser with water.

5. Dual-source heat pump redesign and future work

Based on the results and the problems encountered during the testing of the DSHP, a new design has been carried out and a new prototype has been built. The unit includes a more compact DSHX, based reduced diameters for the tubes and internally enhanced external tubes. This change has allowed an important reduction of the DSHX volume, and thus, the refrigerant charge has been reduced by 70%.

The refrigerant circuit has been optimized, also focusing on the compactness of the unit. It has been simplified, especially regarding the DSHX inlet and outlet parts, as during the experimental campaign of the first prototype an excessive pressure drop was measured in evaporator mode.

Fig. 21 shows the second manufactured prototype, which will be tested in an experimental campaign analogous to the one carried out with the first prototype. Additionally, combined air-water modes in the DSHP (air and water as a source or sink simultaneously in the DSHX) are planned for testing, in order to explore the whole set of possibilities which the DSHX can offer.

Fig. 21 – Second prototype of the DSHP.

The experimental results of the DSHP and the new designed unit will be used to evaluate the energy performance of the whole system, which is focused in multi-family buildings and designed in order to achieve a high renewable share.

6. Acknowledgement

The authors are grateful for the funding received from the EU Horizon 2020 program, within contract no. 814888, corresponding to the TRI-HP project "Trigeneration systems based on heat pumps with natural refrigerants and multiple renewable sources." in which this analysis is framed.

https://www.tri-hp-.eu

7. References

[1] Roadmap to a Resource Efficient Europe. Available at: https://eur-lex.europa.eu/legal-content/EN/TXT/PDF/?uri=CELEX:52011DC0571&from=EN

[2] EU F-Gas Regulation Handbook, EIA, 2015.

[3] Rees, Advances in ground-source heat pump systems. Woodhead Publishing, 2016.

[4] Jin, T. M. Eikevik, P. Nekså, and A. Hafner, "A steady and quasi-steady state analysis on the CO2 hybrid ground-coupled heat pumping system," International Journal of Refrigeration, vol. 76, pp. 29 – 41, 2017.

[5] Man, H. Yang, and J. Wang, "Study on hybrid ground-coupled heat pump system for air-conditioning in hot-weather areas like hong kong," Applied Energy, vol. 87, no. 9, pp. 2826 – 2833, 2010.

[6] Engineering Equation Solver. F-Chart Software. http://www.fchart.com

[7] W. Chi-chuan, H. Yi-chung, and L. Yur-tsai, "Convective heat transfer for plain ns. performance of plate finned tube heat exchangers under dehumidifying conditions," Journal of Heat Transfer, vol. 119/1, pp. 109 – 117, 1997.

[8] Shah, R., London, A., Heat transfer in pipe flow. laminar flow forced convection in ducts, Academic Press, vol. 192, p. 98, 1978.

[9] Nellis, G., Klein, S., Heat Transfer. Cambridge University Press, 2008.

[10] V. D. Ingenieure, VDI-Heat Atlas. Springer, 1993.

[11] Incropera, F., DeWitt, P., David, P., Fundamentals of Heat and Mass Transfer, 6th ed. New York Wiley, 2007.

[12] Shah, M., Comprehensive correlations for heat transfer during condensation in conventional and mini/micro channels in all orientations, International Journal of Refrigeration, vol. 67, pp. 22–41, 2016.

[13] Shah, M., Prediction of heat transfer during condensation in inclined plain tubes, Applied Thermal Engineering, vol. 94, pp. 82–89, 2016.

[14] L. Sun and K. Mishima, An evaluation of prediction methods for saturated _ow boiling heat transfer in minichannels, International Journal of Heat and Mass Transfer, vol. 52, pp. 5323 – 5329, 2009.

[15] Shah, M. M. Chart correlation for saturated boiling heat transfer: equations and further study, ASHRAE Transactions, vol. 88, pp. 185 – 196, 1982

[16] EN 14511-3:2018 Air conditioners, liquid chilling packages and heat pumps for space heating and cooling and process chillers, with electrically driven compressors - Part 3: Test methods.

Data Statement

The datasets generated during and/or analysed during the current study are not publicly available at the moment of the publication of the paper, but will be available under the TRI-HP Data Research Community in Zenodo in the near future. TRI-HP Research Data Community | Zenodo